

# JAAS

Journal of Analytical Atomic Spectrometry

Accepted Manuscript

This article can be cited before page numbers have been issued, to do this please use: M. Horstmann, R. Gonzalez de Vega, D. P. Bishop, U. Karst, P. Doble and D. Clases, *J. Anal. At. Spectrom.*, 2021, DOI: 10.1039/D0JA00493F.



This is an Accepted Manuscript, which has been through the Royal Society of Chemistry peer review process and has been accepted for publication.

Accepted Manuscripts are published online shortly after acceptance, before technical editing, formatting and proof reading. Using this free service, authors can make their results available to the community, in citable form, before we publish the edited article. We will replace this Accepted Manuscript with the edited and formatted Advance Article as soon as it is available.

You can find more information about Accepted Manuscripts in the [Information for Authors](#).

Please note that technical editing may introduce minor changes to the text and/or graphics, which may alter content. The journal's standard [Terms & Conditions](#) and the [Ethical guidelines](#) still apply. In no event shall the Royal Society of Chemistry be held responsible for any errors or omissions in this Accepted Manuscript or any consequences arising from the use of any information it contains.

# Determination of Gadolinium MRI contrast agents in fresh and oceanic waters of Australia employing micro-solid phase extraction, HILIC-ICP-MS and bandpass mass filtering

View Article Online  
DOI: 10.1039/DOJA00493F

Maximilian Horstmann<sup>1,2</sup>, Raquel Gonzalez de Vega<sup>1</sup>, David. P. Bishop<sup>1</sup>, Uwe Karst<sup>2</sup>, Philip A. Doble<sup>1</sup>, David Clases<sup>1\*</sup>

<sup>1</sup> The Atomic Medicine Initiative, University of Technology Sydney, 15 Broadway, Ultimo NSW 2007, Australia

<sup>2</sup> University of Münster, Institute of Inorganic und Analytical Chemistry, Corrensstr. 30, 48149 Münster, Germany

\*corresponding author: email: David.Clases@uts.edu.au

**Abstract:** Gd-based contrast agents (GBCAs) are frequently administered to patients for magnetic resonance imaging to enhance tissue contrasts. After examination, they are excreted and enter surface waters via local wastewater treatment plants' effluents where they lead to anthropogenic Gd anomalies in the environment of metropolitan areas with developed healthcare. This work presents the speciation analysis of GBCAs in water samples from Australia by targeting individual GBCAs in effluent, river and seawater samples obtained from New South Wales (Sydney), the Northern Territory (Alice Springs) and Victoria (Melbourne). A method based on hydrophilic interaction liquid chromatography (HILIC) coupled to inductively coupled plasma - mass spectrometry (ICP-MS) provided rapid separation and quantification of four common GBCAs in under three minutes. To improve the sensitivity, ion extraction and transport processes were optimised, and the quadrupole mass filter was operated with an increased mass bandpass, decreasing limits of detection to between 18 and 24 ng/L for individual GBCAs. This allowed detection of Gd-DOTA, Gd-BT-DO3A and Gd-DTPA-BMA at concentrations of up to 160 ng/L in water samples collected from rivers within the proximity of effluents of local wastewater treatment plants. The analysis of GBCAs in oceanic sea water required the development of a novel automated micro-solid phase extraction ( $\mu$ SPE) method for matrix elimination and analyte pre-concentration enabling the detection of Gd-DOTA and Gd-BT-DO3A.

**Keywords:** Gadolinium anomaly, HILIC-ICP-MS, hard extraction, bandpass mode, solid phase extraction, speciation analysis

## Introduction

Worldwide, an increasing number of more than 30 million magnetic resonance imaging (MRI) examinations per year require Gadolinium-based contrast agents (GBCAs). Since the introduction of gadopentetate dimeglumine into clinical practice in 1988, a variety of Gd complexes have been developed to improve diagnostic imaging capabilities,<sup>1</sup> from which the most frequently administered chelates are depicted in Figure 1. After MRI examination, GBCAs are excreted mostly unmetabolised and enter surface waters unaltered via effluents of local wastewater treatment plants.<sup>2-5</sup> The frequent use of GBCAs resulted in a substantial discharge into the environment causing anthropogenic Gd anomalies, which are defined as elevated Gd levels relative to other naturally abundant lanthanides. These anomalies are often assessed by normalising concentrations of rare earth

elements in waters against a reference material (e.g., shales).<sup>6</sup> Anomalies have been detected in waters around metropolitan areas with developed healthcare.<sup>7-14</sup> In Australia, more than 1 million MRI examinations were conducted in 2017<sup>15,16</sup> and

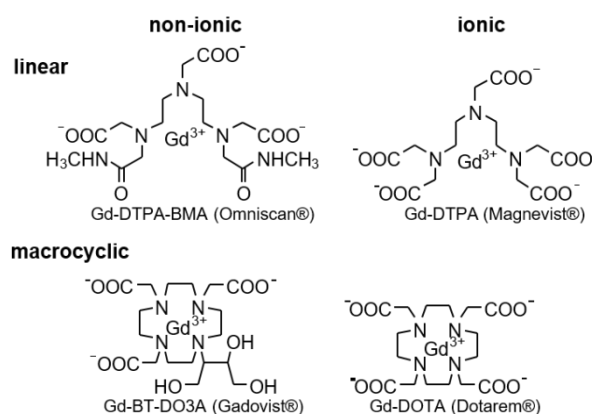


**Figure 1.** Structures of the four most administered GBCAs. Top: linear chelates, Gd-DTPA-BMA and Gd-DTPA; bottom: macrocyclic complexes Gd-DOTA and Gd-BT-DO3A.

1 a Gd anomaly was reported in Brisbane  
2 (Queensland, Australia) in 2009.<sup>17,18</sup>

3  
4 70% of the Australian population live within ten  
5 urban areas,<sup>19</sup> all located on the coast, of which  
6 Greater Sydney and Melbourne are the largest. In  
7 these areas, approximately 10 million people  
8 produce more than 2 billion litres of wastewater  
9 daily which is predominantly diffused into the  
10 South Pacific Ocean via outfalls. However, a small  
11 portion of treated wastewater is discharged into  
12 surrounding river and creek systems. This  
13 complicates speciation analysis as established  
14 methods and sampling strategies are often not  
15 applicable and quantification and selectivity are  
16 impaired due to trace concentrations and complex  
17 matrices. Specifically, speciation analysis in  
18 saltwater is challenging and requires dedicated  
19 pre-treatment as well as detection capabilities to  
20 determine individual Gd species. The (eco-  
21)toxicological impact of GBCAs is difficult to  
22 estimate due to lack of studies investigating the  
23 behaviour of these compounds in the aquatic  
24 environment. Research on the fate,  
25 bioaccumulation, metabolism, and degradation of  
26 Gd complexes is still in an early stage and relies  
27 upon extremely sensitive and selective techniques  
28 that allow differentiation between species in  
29 complex environmental and biological matrices. It  
30 has been previously reported by laser ablation-  
31 inductively coupled plasma-mass spectrometry  
32 (LA-ICP-MS) that Gd from GBCAs may be retained  
33 in the body after MRI examination<sup>20,21</sup>, and Lingott  
34 et al. found that GBCAs in surface waters may be  
35 taken up and accumulate in plants and animals.<sup>22</sup>

36  
37  
38  
39  
40 Positive Gd anomalies in surface and tap waters in  
41 densely populated regions were first identified by  
42 Bau and Dulski in 1996.<sup>1</sup> Since then, methods for  
43 the speciation of Gd have been developed and  
44 refined by hyphenation of  
45 chromatographic/electrophoretic separation  
46 techniques with ICP-MS, which is now a platform  
47 technology for trace analyses of soluble element  
48 species.<sup>2</sup> Polar or/and ionic species including  
49 GBCAs can be separated by ion chromatography,<sup>3</sup>  
50 capillary electrophoresis<sup>4</sup> or hydrophilic interaction  
51 liquid chromatography (HILIC).<sup>5</sup> HILIC-ICP-MS  
52 has been demonstrated to be the gold standard for  
53 efficient separation and sensitive detection of  
54 GBCAs in environmental samples.<sup>6</sup> Several  
55 reviews have been published since the inception of  
56 environmental Gd speciation, where the interested  
57 reader will find further information, applications  
58 and comparisons.<sup>6-8</sup> Using HILIC-ICP-MS,  
59 Künemeyer et al. investigated the distribution of  
60 commonly administered GBCAs in hospital  
effluents, municipal sewage and wastewater with

limits of detection (LODs) as low as 160 ng(Gd)/L.<sup>9</sup>  
Telgmann et al. investigated the concentrations of  
these compounds in wastewater and balanced the  
flux of Gd in a wastewater treatment plant over  
seven days demonstrating that only 10 % of Gd  
was removed during the treatment process (LOD:  
130 ng/L).<sup>10</sup> The figures of merit of GBCAs have  
been incrementally improved to enable detection in  
larger water bodies and complex matrices after  
significant dilution. Lindner et al. analysed GBCAs  
in surface waters and plant extracts with a reported  
LOD of 51 ± 11 ng/L.<sup>11</sup> Using a similar method,  
Raju et al. analysed five GBCAs in surface waters  
in the Berlin area with LODs of 22 ± 5 ng(Gd)/L.<sup>12</sup>  
Birka et al. decreased LODs further by employing  
ultrasonic nebulisation in conjunction with HILIC-  
ICP-sector field-MS reporting LODs of between 1.3  
and 2.2 ng/L allowing quantitative speciation  
analysis in drinking water.<sup>13</sup> Similar figures of merit  
were obtained by Lindner et al. who determined  
GBCAs in tap water samples from the Berlin area  
(LOD: 1,4-2,4 ng(Gd)/L).<sup>14</sup> Okabayashi et al.  
recently demonstrated that HILIC separation may  
be further improved by separating 6 contrast  
agents in less than 800 seconds reaching  
detection limits between 3.4 and 22 ng(Gd)/L.<sup>15</sup>  
Interestingly, the authors presented a HILIC  
approach that did not require organic solvents.  
Decreasing the separation times and consequently  
accelerating the sample throughput will become  
increasingly important for larger programs of close  
meshed tracing of various samples in larger water  
bodies. However, while figures of merit  
incrementally improved over time, methods for  
speciation analysis in complex matrices like  
seawater have not been developed.

This work presents a novel automated micro-solid  
phase extraction ( $\mu$ SPE) method to eliminate  
complex matrixes and pre-concentrate GBCAs  
from seawater. Speciation was performed using a  
rapid HILIC-ICP-MS method which featured  
improved ion transmission by modifying ion  
extraction, transport and increasing the  
quadrupole's mass bandwidth to improve LODs.

## Materials and Methods

Ultrapure water was obtained from an Arium® pro  
system from Sartorius Stedim Biotech (18.2 M $\Omega$ ,  
Göttingen, Germany). Acetonitrile (HPLC grade)  
and ammonium acetate were purchased from  
Sigma Aldrich (St. Louis, USA). High purity Gd  
standards for ICP-MS were obtained at 10 mg/L  
from Choice Analytical (Thornleigh, New South  
Wales, Australia). All contrast agents were  
acquired from their respective pharmaceutical  
suppliers: Magnevist® (Gd-DTPA, 0.5 mol/L) and

Gadovist® (Gd-BT-DO3A, 1.0 mol/L) from Bayer Pharma AG (Berlin, Germany), Dotarem® (Gd-DOTA, 0.5 mol/L) from Guerbet SA (Villepinte, France) and Omniscan® (Gd-DTPA-BMA, 0.5 mol/L) from GE Healthcare (Chalfont St Giles, United Kingdom). 0.45 µm PTFE syringe filters were purchased from Tisch Scientific (North Bend OH, USA). Water samples were kept in containers made of polypropylene to avoid adsorption effects of GBCAs. µSPEed cartridges containing µCarb resin (porous graphitic carbon, 3 µm, 250 Å) were obtained from ePrep Pty Ltd (Mulgrave Vic, Australia).

### Sample and standard preparation

Samples were collected in 50 mL polypropylene containers previously washed with the sampling matrix. The sampling locations, times and descriptions are listed in Table 1. All samples were filtered to remove larger particles and stored at -20 °C until analysis. For analysis, samples were left at room temperature until thawed and diluted 1:10 in eluent. For the construction of calibration curves and species identification, GBCA standards were diluted in water and acetonitrile (eluent composition) to concentrations of 10, 100, 1,000 and 10,000 ng/L. Ultrapure water was used to obtain a blank value. GBCA standards were cross-calibrated using a certified Gd standard for ICP-MS. The standard solutions containing Gd-DTPA, Gd-DOTA, Gd-BT-DO3A and Gd-DTPA-BMA were prepared daily to prevent metal exchange with excess ligands present in the formulations.

For speciation analysis in seawater, an automated µSPE method was developed. Method development was carried out on a digiVOL® Programmable Digital Syringe Driver (ePrep Pty Ltd, Mulgrave Vic, Australia) with µCarb µSPEed® extraction cartridges. For automation, the method

was transferred to a Sample Preparation Workstation (ePrep Pty Ltd, Mulgrave Vic, Australia). The workflow for the preparation/pre-concentration of GBCAs from seawater is illustrated in Figure 2. Syringes made of glass were treated with HNO<sub>3</sub> and flushed with ultrapure water to mitigate GBCA carryover. The absence of contaminating GBCAs was regularly checked by preparing and analysing blank solutions. µSPEed® cartridges were conditioned with ultrapure water to activate the carbon surface, loaded with sample volumes between 250 and 1000 µL and eluted with 250 µL (73% acetonitrile, 27% MQ water). The dispensing flow rate for the elution step was optimised to 500 µL/min, while 1000 µL/min was used for the conditioning, loading and washing steps. The entire µSPE workflow including syringe cleaning required approximately 15 minutes per sample. As a method blank and medium for spiking experiments, seawater was obtained approximately 30 km outside the metropolitan area of Sydney where no anomaly was expected (-34.116363, 151.140778). Known concentrations of Gd-DTPA, Gd-DOTA, Gd-BT-DO3A and Gd-DTPA-BMA were spiked into the seawater blank and analysed by µSPE and HILIC-ICP-MS to determine recoveries.

### Instrumentation

Chromatographic separations were performed on a 1200 series HPLC system (Agilent Technologies) using an Accucore™ HILIC silica LC-column (dimensions 100 x 2.1 mm, particle size 2.6 µm, Thermo Fisher Scientific) equipped with an Accucore™ HILIC defender guard (dimension 10 x 2.1 mm, particle size 2.6 µm). The starting point for the optimisation of the separation method were chromatographic conditions reported

**Table 1.** Sampling location, date, time, and description. All sample are associated with WWTP discharges after tertiary treatment.

Location	Date Time	Description	Latitude Longitude
1	15/06/2018 10:44 AM	Downstream of WWTP (Discharge: 32.6 ML/d)	-33.7365 150.8750
2	15/06/2018 01:08 PM	Downstream of WWTP (Discharge: 0.9 ML/d)	-33.5750 150.7167
3	15/06/2018 10:53 AM	Downstream of WWTP (Discharge: 11.9 ML/d)	-33.7013 151.0831
4	15/06/2018 11:20 AM	Downstream of WWTP (Discharge: 24 ML/d)	-33.6673 150.9210
5	15/06/2018 03:00 PM	Downstream of WWTP (Discharge: 60 ML/d)	-33.7142 150.7671
6	15/06/2018 02:17 PM	Downstream of WWTP (Discharge: 24 ML/d)	-33.7419 150.6924
7	21/10/2019 03:11 PM	WWTP effluent (seepage) (Discharge: n/a)	-23.73637 133.8586
8	10/12/2019 04:34 PM	WWTP effluent diffused in seawater (Discharge: 330 ML/d)	38.4405 144.8474

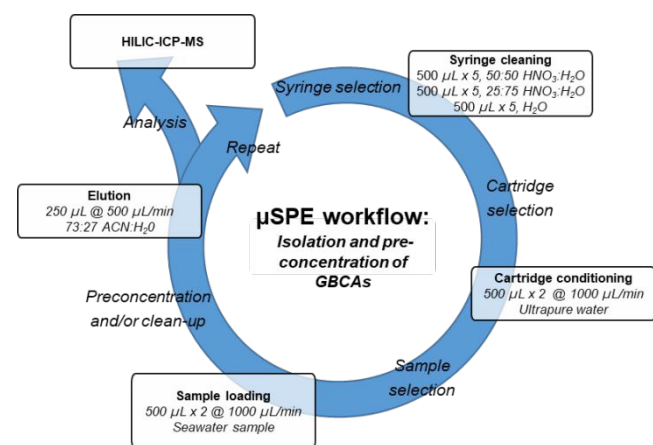


**Figure 2.** µSPE workflow for the preconcentration and clean-up of GBCAs from seawater. Without preconcentration, the sample loading volume was reduced to 250 µL.

by Birka et al. in 2013.<sup>27</sup> To accelerate the separation of GBCAs, the dimensions of the chromatographic column were altered (150 x 3 mm, 2.1  $\mu\text{m}$   $\rightarrow$  100 x 2.1 mm, 2.6  $\mu\text{m}$ ) while increasing the flow rate to 1.1 mL/min. Furthermore, a higher content of acetonitrile (eluent A: 30% 10 mM ammonium acetate buffer solution in ultrapure water and 10% acetonitrile, eluent B: 70% acetonitrile, isocratic conditions) was used and, the column temperature was set to 40°C to reduce the backpressure. Different pH values (2-8) of the aqueous eluent (prior to adding acetonitrile) and effects regarding peak shape and separation efficiencies were investigated until finding an optimum at a pH value of 5.3. These optimised parameters reduced the separation time from previously approximately 14 minutes to less than three minutes.<sup>27</sup> The optimum injection volume was determined empirically to be 5  $\mu\text{L}$  while considering peak symmetries and signal to noise ratios. Before each injection, the column was equilibrated for at least 3 minutes.

A 7700 series ICP-MS system (Agilent Technologies) was equipped with platinum cones, cs lenses and a narrow injector (1 mm) torch and operated with MassHunter software (Agilent Technologies). A method with an increased mass bandpass further referred to as bandpass mode was used to improve sensitivity and analysed Gd at 156 amu. The dwell time was set to 100 ms, and 163 amu, 148 amu and 140 amu were monitored additionally to ensure the absence of spectral interferences from other lanthanides. For comparisons, <sup>158</sup>Gd was monitored employing a standard method. A 20% oxygen/argon blend was added through a T-piece before the torch to mitigate carbon deposition on the interface (tuning value: 25%). A Scott-type double-pass spray chamber (Glass Expansion, West Melbourne, Victoria, Australia) was cooled to -5 °C and a MicroMist™ concentric nebuliser (Elemental Scientific, Omaha, NE, USA) was used for sample nebulisation. The performance of the ICP-MS instrument was tuned daily with a solution (70: 30, acetonitrile: water) containing 1  $\mu\text{g/L}$  Li, Y, Tl and Ce to optimise sensitivity. The CeO/Ce signal was used to determine the oxide rate which was below 5%. The signal to noise ratio for the analysis of Gd was further optimised analysing a diluted 1  $\mu\text{g/L}$  element standard (70: 30, acetonitrile: water). The plasma was operated at 1.6 kW and the typical nebuliser gas and make-up gas flow rates were tuned daily to a total gas flow rate of between 0.7 and 0.8 L/min.

**Table 2.** Instrumental parameters of a standard method (SM) and for a method operating the quadrupole with an increased mass bandwidth (bandpass mode (BPM)).

Tune mode	SM	BPM
	Monitored at [amu]	158
<b>Lenses</b>		
Extr. Lens 1 [V]	4.0	-80.0
Extr. Lens 2 [V]	-150	-5.0
Omega Bias [V]	-32	-150
Omega Lens [V]	8.6	24.4
Deflect [V]	17.0	20.0
<b>Cell</b>		
He Flow [mL/min]	0	0.5
H <sub>2</sub> Flow [mL/min]	0	0.5
Octopole Bias [V]	-6.0	-18.0
Octopole RF [V]	150	13
Energy Discr. [V]	4.0	-3.3
<b>Quadrupole</b>		
Mass Gain [V]	127	30
Mass Offset [V]	129	111

The bandpass mode was developed stepwise by first increasing ion transmission through manipulation of extraction and ion transport conditions. In a second step, the mass bandwidth of the quadrupole mass filter was increased. The bandwidth and mass resolution of a quadrupole are set by the combination of direct current (DC) voltage and RF voltage applied to the four rods. The pairs of RF and DC voltages applied are located on one scan line which is defined via a linear function that can be altered by a set of tune parameters. In this case, the scan line function was altered by manipulation of the tune values "Mass Gain" and "Mass Offset". Various combinations of these tune parameters were evaluated for signal to noise ratios of Gd. The optimised experimental parameters for the standard method and the bandpass mode are listed in Table 2.

The advantages of cell gas (He and H<sub>2</sub>) were further investigated as part of the tuning process. The flow rates of these gases were optimised by analysing a 1  $\mu\text{g/L}$  Gd standard diluted in eluent and by comparing the Gd signal to the background monitored outside Gd's mass bandpass. The operation of low cell gas flows reduced the background noise without significantly affecting the sensitivity of Gd leading to improved signal to

1 noise ratios. Furthermore, the application of cell  
2 gases appeared to improve the Gd signal stability.

### 3 Data handling and figures of merit

4 Data was processed with Origin (OriginLab  
5 Corporation, Northampton, USA). Chromatograms  
6 were smoothed using a Savitzky-Golay filter over  
7 15 data points. The  $\mu$ SPE recoveries for each  
8 compound were determined analysing a 1000 ng/L  
9 GBCA calibration standard mix via HILIC-ICP-MS  
10 without  $\mu$ SPE, after  $\mu$ SPE (no preconcentration)  
11 and after  $\mu$ SPE with a preconcentration factor of 4.  
12 Column recoveries were calculated by subsequent  
13 comparison to flow injection (FI) ICP-MS. The FI  
14 method operated the described LC method without  
15 the column and was used to determine the peak  
16 area for each GBCA standard individually. The  
17 peak area determined by FI-ICP-MS was used to  
18 normalise the detected area in HILIC-ICP-MS to  
19 obtain the recoveries. Limits of detection (LODs)  
20 and limits of quantification (LOQs) were calculated  
21 based on the integral's standard deviation (noise)  
22  $\sigma$  of a calibration blank and the slope (sensitivity,  
23  $s$ ) of the respective calibration curves (LOD = 3  
24  $\sigma/s$ , LOQ = 10  $\sigma/s$ ). Analyses were performed in  
25 triplicate to obtain the standard deviation.

## 26 **Results and discussion**

### 27 Increasing ion transmission

28 The sensitivity of ICP-MS is dependent on the ion  
29 transport efficiency, which can be increased by  
30 several strategies. One involves the use of hard  
31 extraction conditions operating the first extraction  
32 lens with a highly negative potential and the  
33 second extraction lens closer to the ground  
34 potential. This increases the kinetic energy of  
35 extracted ions, which translates into an increased  
36 ion transmission visible as increased sensitivity in  
37 ICP-MS. However, background noise and  
38 interferences must be monitored closely, as noise  
39 usually increases concomitant with ion  
40 transmission. If noise increases to a similar extent,  
41 signal to noise ratios may deteriorate and LODs  
42 increase. The manipulation of extraction potentials  
43 is a common approach for sector-field ICP-MS and  
44 have also been reported for quadrupole-based  
45 ICP-MS, for example in single particle ICP-MS<sup>36</sup>,  
46 LA-ICP-MS<sup>37</sup> or gas chromatography (GC)-ICP-  
47 MS<sup>38</sup>. However, consideration of the downstream  
48 effects is required to optimise the working range of  
49 the remaining ion lenses. For example, a curvature  
50 of the ion beam is usually induced to eliminate  
51 neutral particles and light. Increasing the kinetic  
52 energies may require altering electric potentials to  
53 maintain and focus of this ion trajectory.

Another strategy to increase ion transmission  
involves modification of the quadrupole scanning  
parameters. Similar approaches were previously  
described for ICP-MS/MS to increase the ion  
transmission of the first quadrupole, and we  
recently investigated this concept for single  
quadrupole ICP-MS instruments.<sup>36,37,39,40</sup> In  
conventional quadrupole-ICP-MS,  $m/z$  are  
scanned sequentially and therefore, sensitivity is  
lower for elements with a broad and even isotope  
distribution when compared with a monoisotopic  
element. This applies specifically to Gd, which  
consists of 7 isotopes with abundances between  
0.2% and 24.84% as shown in Figure 3C.  
Therefore, analysing the most abundant isotope  
<sup>158</sup>Gd limits measurement to a small fraction of the  
overall Gd, and more than 75% of all Gd ions  
transmitted to the quadrupole are subsequently  
eliminated. Ions with different  $m/z$  follow individual  
trajectories within the quadrupole and the  
combination of DC voltage and RF voltage applied  
to the rods determines whether the ion trajectory is  
stable and focusses onto the detector. Each  $m/z$   
has a stability zone which can be calculated by  
solving the Mathieu equations. Figure 3A shows  
exemplary stability zones of three  $m/z$  in which any  
combination of DC and RF voltage produce stable  
trajectories. However, to maintain a consistent  
(unit) mass resolution and ion transmission, only  
specific pairs of DC and RF voltages are applied  
and are located on one line (scan line 1, Figure  
3A).

Modification of the gain and slope of the scan line  
(compare scan line 2, Figure 3A) increases  
transmission of individual high-mass isotopes as  
exemplified in Figure 3B. Furthermore, due to the  
decreasing mass resolution, the mass peak width  
of each isotope increases to approximately 8 amu  
causing a convolution of isotopic signals as shown  
in Figure 3D. The signal convolution allows  
transmission of several isotopes simultaneously  
while applying only one set of RF and DC voltages  
to the quadrupole, and consequently increases  
sensitivity further. Figure 3E shows a simulated  
mass spectrum demonstrating the isotope signal  
convolution where individual isotope signals are  
stacked and Figure 3F shows a measured mass  
spectrum of Gd employing a standard method  
(red) and the bandpass mode (blue). The  
increased ion transmission of the bandpass mode  
for individual isotopes and the signal convolution  
increased sensitivity by a factor of 44 compared  
against the standard method monitoring the most  
abundant Gd isotope (<sup>158</sup>Gd, 24.84%).

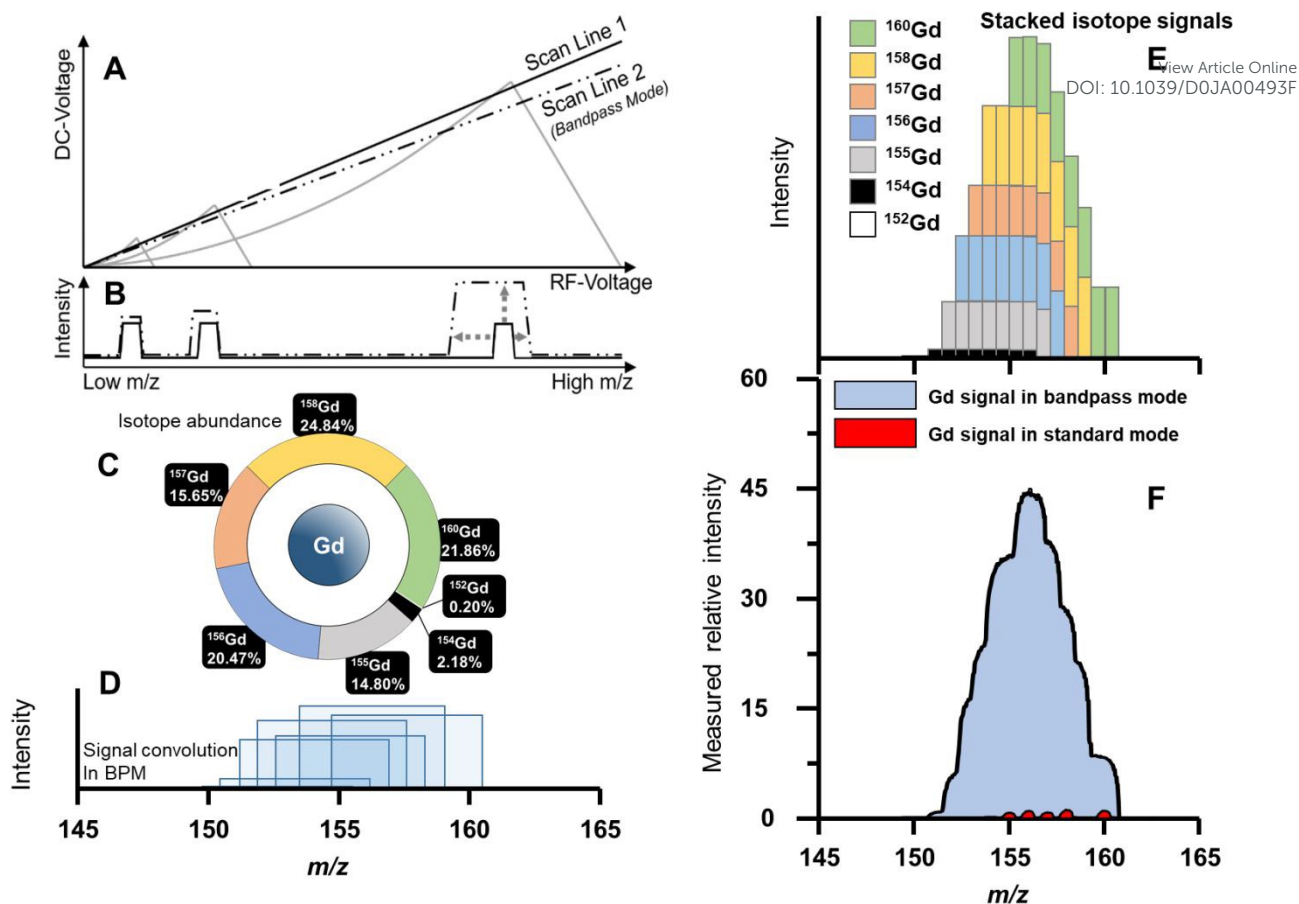


**Figure 3.** **A:** Stability diagram for three  $m/z$  representing low, mid and high masses. Scan line 1 truncates the three stability zones to provide uniform mass resolution and ion transmission over the entire mass scale. Ion transmission and mass resolution may be modified by manipulation of the scan line function (compare scan line 2). **B:** Applying scan line 2 increases ion transmission for heavy masses and results in larger mass peak widths. **C:** Isotopic abundance of Gd. With a standard mode, highest sensitivity for Gd is achieved at 158 amu. **D:** Manipulation of the scan line changes the transmission and mass resolution leading to a convolution of isotopic signals. **E:** Stacked simulation of individual isotopic signals. Broad peak widths and signal convolution allows the analysis of several isotopes simultaneously further increasing sensitivity. **F:** Comparison of measured mass signals obtained from a standard mode with unit mass resolution and the bandpass mode.

For the samples investigated in this study, co-eluting interferences (e.g., other lanthanides or polyatomic interferences) were unlikely. However, depending on the application, large mass bandpass filtering requires consideration of potential spectral overlaps of targeted isotopes and potentially interfering compounds. This may become increasingly relevant when other lanthanide anomalies are present as for example described by Kulaksiz and Bau.<sup>16</sup> Increasing sensitivity by increasing the mass bandwidth of the quadrupole decreases mass selectivity. While the loss of unit mass resolution contributes to the improved ion transmission and isotope signal convolution which increases sensitivity, it becomes more difficult to distinguish Gd from other adjacent lanthanides and polyatomic interferences. At the same time, background noise may increase and limit the gain in signal to noise ratios and improvement in LODs. It is noteworthy that the

mass bandwidth broadens asymmetrically. For example, increasing the mass bandwidth of an isotope with  $m/z$  159 from 1 amu to 8 amu did not produce a mass signal that was symmetrically centred around 159 amu with  $\pm 4$  amu. Instead, the mass signal was shifted towards lower masses with signal boundaries at approximately 152.5 and 160.5 amu. This is a direct consequence of asymmetric stability zones shown in Figure 3A and is relevant for consideration of potential isobaric and polyatomic interferences, which may affect accuracy when operating a large mass bandpass. In this case, monitoring Gd at 156 amu achieved the highest sensitivity and prevented interferences from lighter lanthanide isotopes like <sup>153</sup>Eu. However, a spectral overlap with isotopes from <sup>159</sup>Tb, <sup>162</sup>Er, <sup>156</sup>Dy, <sup>158</sup>Dy, <sup>160</sup>Dy, <sup>161</sup>Dy and <sup>162</sup>Dy was possible and was investigated to ensure accuracy. The impact of Er and Dy on the Gd signal was evaluated by monitoring 163 amu

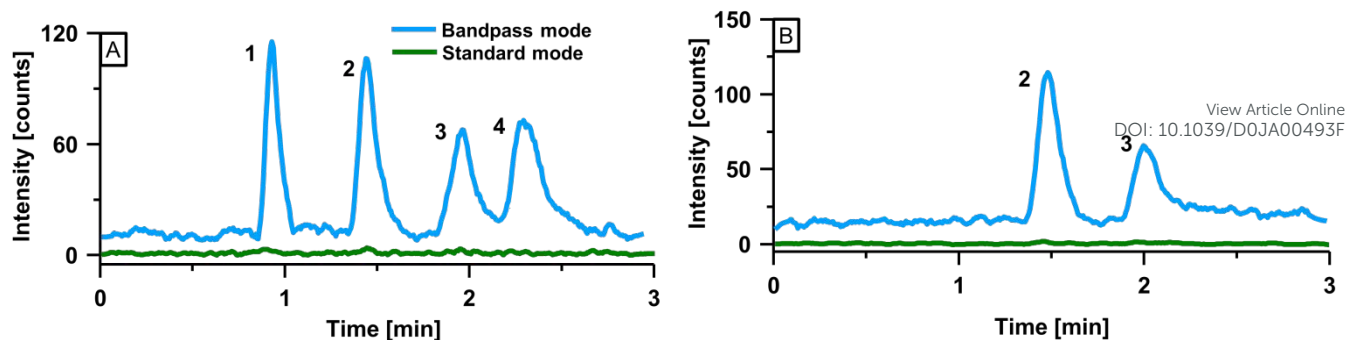


**Figure 4. A:** Separation of a 100 ng/L mix containing the 4 most frequently administered GBCAs (1: Gd-DTPA, 2: Gd-DOTA, 3: Gd-BT-DO3A, 4: Gd-DTPA-BMA). Two methods were used for signal acquisition: a standard method with soft extraction conditions (green), and a bandpass mode method (blue). **B:** Chromatographic separation of a riverine sample obtained in the Sydney region (location 4) employing the standard and bandpass mode.

additionally to 156 amu. To recognise the potential impact of lighter isotopes forming polyatomic interferences (e.g.,  $^{140}\text{Ce}^{16}\text{O}$ ), 140 amu and 148 amu were also monitored. Furthermore, all samples investigated in the framework of this study were first analysed via FI-ICP-MS to screen for lanthanides using a standard method and no significant signals for any lanthanide potentially interfering with Gd were found. To prevent potential polyatomic interferences and to reduce background noise, He and  $\text{H}_2$  were used as cell gases.

### Speciation analysis in surface waters

A standard mix containing the four GBCAs was diluted to 100 ng/L and analysed by HILIC-ICP-MS employing a standard method and the bandpass mode, respectively. Figure 4A (blue) shows the resulting chromatogram demonstrating rapid separation of all four GBCAs in below three minutes. The figures of merit of for both methods and each GBCA are shown in Table 3. The  $R^2$  values were determined as a measure of linearity and were at least 0.9997. The column recovery was 104% for Gd-DTPA, 105% for Gd-DOTA, 70%

for Gd-BT-DO3A and 89% for Gd-DTPA-BMA. The LODs and LOQs of GBCAs acquired with the standard method were between 100 - 120 ng/L and 320 - 410 ng/L, respectively and were in agreement with previous studies using similar instrumentation.<sup>4,30</sup> Accordingly, individual GBCAs were not detected analysing a 100 ng/L calibration standard as shown in Figure 4A (green). The manipulation of ion extraction and transport and operating the quadrupole in bandpass mode increased sensitivity by a factor of between 43 and 50 for the individual GBCA while increasing background noise by a factor of less than 10 (compare Table 3). The increases in sensitivity were in line with values obtained analysing Gd via standalone ICP-MS shown in Figure 3F. Consequently, LODs and LOQs decreased to 20 and 67 ng/L for Gd-DTPA, 18 and 60 ng/L for Gd-DOTA, 24 and 81 ng/L for Gd-BT-DO3A and 21 and 71 ng/L for Gd-DTPA-BMA allowing the detection and quantification of all four GBCAs as shown in Figure 4A (blue). The improved figures of merit were crucial for the detection of GBCAs in surface waters of Sydney (Australia). Sample locations 1-5 (compare Table 1) were located

**Table 4.** Concentrations of GBCAs in all freshwater samples. All concentrations are in ng/L. GBCAs below the LOD were labelled as “not detected (*n.d.*)” and GBCAs determined between the LOD and LOQ are labelled as “<LOQ”.

Location	Gd-DTPA	Gd-DOTA	Gd-BT-DO3A	Gd-DTPA-BMA
1	<i>n.d.</i>	<LOQ	160±5	<i>n.d.</i>
2	<i>n.d.</i>	<i>n.d.</i>	<i>n.d.</i>	<i>n.d.</i>
3	<i>n.d.</i>	<i>n.d.</i>	<i>n.d.</i>	<i>n.d.</i>
4	<i>n.d.</i>	130±5	<LOQ	<i>n.d.</i>
5	<i>n.d.</i>	<LOQ	<i>n.d.</i>	<i>n.d.</i>
6	<i>n.d.</i>	<LOQ	110±3	100±1
7	<i>n.d.</i>	60	<i>n.d.</i>	<i>n.d.</i>

**Table 3.** Figures of merit for each GBCA and method. Methods using standard method (SM) and a method operating the quadrupole in bandpass mode (BPM) were compared.

Unit		Sensitivity Cts L ng <sup>-1</sup>	Noise Cts	LOD ng/L	LOQ ng/L	R <sup>2</sup>
Gd-DTPA	SM	0.12	4.3	110	350	0.9997
	BPM	6.0	40	20	67	0.9999
Gd-DOTA	SM	0.14	5.3	120	390	1.0000
	BPM	6.6	39	18	60	0.9999
Gd-BT-DO3A	SM	0.12	4.8	120	410	0.9999
	BPM	5.5	45	24	81	1.0000
Gd-DTPA-BMA	SM	0.17	5.3	100	320	0.9999
	BPM	7.4	52	21	71	0.9999



within the greater Sydney region. Most wastewater (approximately 88%) of Sydney is diffused offshore and only a fraction is released into local waterways. Consequently, concentrations of GBCAs are low and speciation analysis required sensitive methods. Figure 4B shows the speciation analysis of a surface water obtained from a creek in northwest Sydney (location 4). While the standard method was not able to detect GBCAs, operating hard extraction conditions and improving ion transmission by increasing the mass bandpass of the quadrupole allowed the quantification of Gd-DOTA ( $130 \pm 5$  ng/L) and the additional detection of Gd-BT-DO3A (<LOQ). Determined species and concentrations for all locations are listed in Table 4.

### Speciation analysis in seawater

The majority of wastewater in Australian coastal cities are diffused via deep water ocean outfalls into the Pacific Ocean. The speciation analysis of GBCAs in seawater is confounded by the high salt content limiting the applicability of HILIC-ICP-MS. Figure 5 (top) shows the analysis of a standard mix containing four GBCAs at  $1 \mu\text{g/L}$  in seawater (red). It is evident that the high ionic strength of the seawater matrix interfered with the separation mechanism in HILIC and prevented the speciation of individual Gd species. Activated carbon was previously reported to partially remove GBCAs from water resources.<sup>43</sup> In this work, activated carbon was obtained in  $\mu\text{SPEed}^{\text{®}}$  cartridges to achieve automated extraction from seawater. As proof of principle, four GBCAs were spiked into seawater without Gd anomaly ( $1 \mu\text{g/L}$ ), and subsequently extracted using a fully automated method employing a Sample Preparation Workstation (ePrep Pty Ltd) and analysed by HILIC-ICP-MS operating the quadrupole in bandpass mode. Figure 5 (top) shows the resulting chromatogram (grey) and compared it to the direct analysis of the same GBCA in spiked seawater (red). The extraction method was crucial to remove

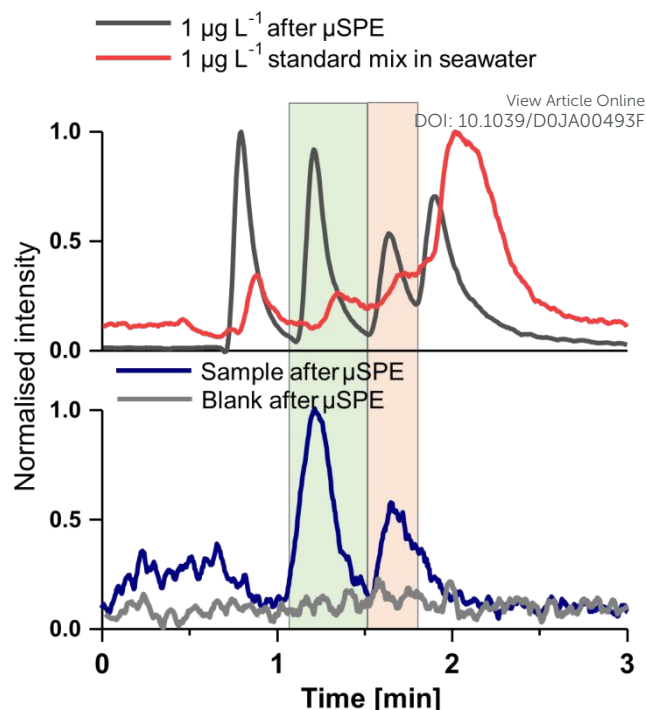


**Figure 5.** Top: HILIC-ICP-MS (bandpass mode) of seawater spiked with a GBCA calibration standard with (grey) and without (red) previous  $\mu\text{SPE}$  (1: Gd-DTPA, 2: Gd-DOTA, 3: Gd-BT-DO3A, 4: Gd-DTPA-BMA). Bottom: Analysis of coastal seawater obtained 700 m offshore of Sydney (location 8). Seawater obtained further away from Sydney was used as

the matrix and allow the separation of individual GBCAs for quantification. The recovery of the developed  $\mu\text{SPE}$  method was determined analysing spiked seawater samples and was between 99.0 and 99.8%. This method was further investigated for its potential to preconcentrate GBCAs. A 4-fold pre-concentration factor was achieved with recoveries between 73.1 and 94.1. The recoveries for each GBCA are listed in Table 5. Figure 5 (bottom) shows the chromatogram of a sample obtained in coastal seawater within the proximity of a wastewater effluent (location 8). Two signals corresponding to Gd-DOTA and Gd-BT-DO3A were detected and calibrated at  $180 \pm 34$  and  $140 \pm 36$  ng/L.

### Conclusion

This work presents the speciation analysis of GBCAs in the Australian environment. Increasing ion extraction and transport and increasing the mass bandwidth of the quadrupole mass filter improved sensitivity by factors of between 43 and 50 relative to a standard method, and decreased LODs and LOQs to between 18 and 24 ng/L and 60 and 81 ng/L, respectively, for the four investigated GBCAs Gd-DTPA, Gd-DOTA, Gd-BT-

**Table 5.** Recoveries after  $\mu\text{SPE}$  without preconcentration and with a preconcentration factor of 4.

Gd species	$\mu\text{SPE}$ recovery	$\mu\text{SPE}$ recover after pre-concentration
Gd-DTPA	$99.8 \pm 8.6$	$73.1 \pm 12.9$
Gd-DOTA	$99.2 \pm 1.3$	$93.5 \pm 5.4$
Gd-BT-DO3A	$99.2 \pm 3.0$	$94.1 \pm 11.7$
Gd-DTPA-BMA	$99.0 \pm 1.0$	$90.0 \pm 8.1$

DO3A and Gd-DTPA-BMA. These improvements allowed the detection and quantification of GBCAs (between 60 and 160 ng/L) found in Australian riverine water samples. A novel automated  $\mu$ SPE method allowed matrix elimination and detection of individual species (Gd-DOTA and Gd-BT-DO3A) in seawater for the first time. The recovery of the GBCAs was between 99.0 and 99.8% without preconcentration and between 73.1 and 94.1% with four-fold preconcentration. These methods have the potential to sufficiently improve figures of merit to trace GBCAs in surface and coastal seawater to monitor the discharge and distribution of GBCAs in the marine environment. The rapid HILIC separation and the fully automated  $\mu$ SPE workflow have further potential for high throughput analyses and to facilitate close-meshed speciation analysis in larger water bodies.

## Author contributions

The manuscript was written through contributions of all authors. All authors have given approval to the final version of the manuscript.

\*Corresponding author:

David Clases, [David.Clases@uts.edu.au](mailto:David.Clases@uts.edu.au)

## Acknowledgements

This research is supported by the UTS Seed Funding scheme.

DPB is supported by an Australian Research Council Discovery Early Career Researcher Award DE180100194.

PAD is supported by Australian Research Council Discovery Project Grant DP190102361.

DC is funded by the Deutsche Forschungsgemeinschaft (DFG, German Research Foundation) - 417283954.

The authors acknowledge the support by ePrep Pty Ltd, Victoria, Australia.

## Conflict of interest

The authors declare no conflicts of interest.

## References

- J. Lohrke, T. Frenzel, J. Endrikat, F. C. Alves, T. M. Grist, M. Law, J. M. Lee, T. Leiner, K.-C. Li, K. Nikolaou, M. R. Prince, H. H. Schild, J. C. Weinreb, K. Yoshikawa and H. Pietsch, *Adv. Ther.*, 2016, **33**, 1–28.
- P. Verlicchi, A. Galletti, M. Petrovic and D. Barceló, *J. Hydrol.*, 2010, **389**, 416–428.
- S. Kulaksiz and M. Bau, *Appl. Geochemistry*, 2011, **26**, 1877–1885.
- L. Telgmann, C. A. Wehe, J. Künemeyer, A. C. Bülter, M. Sperling and U. Karst, *Anal. Bioanal. Chem.*, 2012, **404**, 2133–2141.
- K. Kümmerer and E. Helmers, *Environ. Sci. Technol.*, 2000, **34**, 573–577.
- D. Clases, M. Sperling and U. Karst, *TrAC - Trends Anal. Chem.*, 2018, **104**, 135–147.
- S. Kulaksiz and M. Bau, *Earth Planet. Sci. Lett.*, 2007, **260**, 361–371.
- P. Möller, P. Dulski, M. Bau, A. Knappe, A. Pekdeger and C. Sommer-Von Jarmersted, in *Journal of Geochemical Exploration*, 2000, vol. 69–70, pp. 409–414.
- M. Rabiet, F. Brissaud, J. L. Seidel, S. Pistre and F. Elbaz-Poulichet, *Chemosphere*, 2009, **75**, 1057–1064.
- F. Elbaz-Poulichet, J. L. Seidel and C. Othoniel, *Water Res.*, 2002, **36**, 1102–1105.
- M. Bau, A. Knappe and P. Dulski, *Chemie der Erde*, 2006, **66**, 143–152.
- T. Ogata and Y. Terakado, *Geochem. J.*, 2006, **40**, 463–474.
- P. A. Rinck and R. N. Muller, *Eur. Radiol.*, 1999, **9**, 998–1004.
- D. Clases, M. Sperling and U. Karst, *Trends Anal. Chem.*, 2018, **104**, 135–147.
- “Australia: Total population from 2014 to 2024 (in millions)”, IMF, *online*: <https://www.statista.com/statistics/263740/total-population-of-australia/>, 2019.
- OECD, in *Health at a Glance 2019*, 2019, p. 193.
- M. G. Lawrence, *Mar. Pollut. Bull.*, 2010, **60**, 1113–1116.

- 1 18 M. G. Lawrence, C. Ort and J. Keller,  
2 *Water Res.*, 2009, **43**, 3534–3540.
- 3  
4 19 Australian Bureau of Statistics, 2018.
- 5  
6 20 D. Clases, S. Fingerhut, A. Jeibmann, M.  
7 Sperling, P. Doble and U. Karst, *J. Trace*  
8 *Elem. Med. Biol.*, 2019, **51**, 212–218.
- 9  
10 21 M. Birka, K. S. Wentker, E. Lusmüller, B.  
11 Arheilger, C. A. Wehe, M. Sperling, R.  
12 Stadler and U. Karst, *Anal. Chem.*, 2015,  
13 **87**, 3321–3328.
- 14  
15 22 J. Lingott, U. Lindner, L. Telgmann, D.  
16 Esteban-Fernández, N. Jakubowski and U.  
17 Panne, *Environ. Sci. Process. Impacts*,  
18 2016, **18**, 200–207.
- 19  
20 23 M. Bau and P. Dulski, *Earth Planet. Sci.*  
21 *Lett.*, 1996, **143**, 245–255.
- 22  
23 24 D. P. Bishop, D. J. Hare, D. Clases and P.  
24 A. Doble, *TrAC - Trends Anal. Chem.*,  
25 2018, 104, 11–21.
- 26  
27 25 P. Hajós, D. Lukács, E. Farsang and K.  
28 Horváth, *J. Chromatogr. Sci.*, 2016, **54**,  
29 1752–1760.
- 30  
31 26 J. Künnemeyer, L. Terborg, S. Nowak, L.  
32 Telgmann, F. Tokmak, K. Bernhard, A. Gu,  
33 G. A. Wiesmu, J. Waldeck, C. Bremer and  
34 U. Karst, *Anal. Chem.*, 2009.
- 35  
36 27 M. Birka, C. A. Wehe, L. Telgmann, M.  
37 Sperling and U. Karst, *J. Chromatogr. A*,  
38 2013, **1308**, 125–131.
- 39  
40 28 J. Rogowska, E. Olkowska, W. Ratajczyk  
41 and L. Wolska, *Environ. Toxicol. Chem.*,  
42 2018, **37**, 1523–1534.
- 43  
44 29 L. Telgmann, M. Sperling and U. Karst,  
45 *Anal. Chim. Acta*, 2013, **764**, 1–16.
- 46  
47 30 J. Künnemeyer, L. Terborg, B. Meermann,  
48 C. Brauckmann, I. Möller, A. Scheffer and  
49 U. Karst, *Environ. Sci. Technol.*, 2009, **43**,  
50 2884–2890.
- 51  
52 31 U. Lindner, J. Lingott, S. Richter, N.  
53 Jakubowski and U. Panne, *Anal. Bioanal.*  
54 *Chem.*, 2013, **405**, 1865–1873.
- 55  
56 32 C. S. K. Raju, A. Cossmer, H. Scharf, U.  
57 Panne and D. Lück, *J. Anal. At. Spectrom.*,  
58 2010, **25**, 55–61.
- 59  
60 33 M. Birka, C. A. Wehe, O. Hachmüller, M.  
Sperling and U. Karst, *J. Chromatogr. A*,  
2016, **1440**, 105–111.
- 34 U. Lindner, J. Lingott, S. Richter, W. Jiang,  
N. Jakubowski and U. Panne, *Anal.*  
*Bioanal. Chem.*, 2015, **407**, 2415–2422.  
View Article Online  
DOI: 10.1039/C5AY06493F
- 35 S. Okabayashi, L. Kawane, N. Y.  
Mrabawani, T. Iwai, T. Narukawa, M.  
Tsuboi and K. Chiba, *Talanta*, 2021, **222**,  
121531.
- 36 S. Meyer, R. Gonzalez de Vega, X. Xu, Z.  
Du, P. A. Doble and D. Clases, *Anal.*  
*Chem.*, 2020.
- 37 D. Clases, R. Gonzalez de Vega, S. Funke,  
T. E. Lockwood, M. Westerhausen, R. V.  
Taudte, P. A. Adlard and P. Doble, *J. Anal.*  
*At. Spectrom.*, 2020, **35**, 728–735.
- 38 D. Clases, M. Ueland, R. Gonzalez de  
Vega, P. Doble and D. Pröfrock, *Talanta*,  
2021, **221**, 121424.
- 39 L. Balcaen, G. Woods, M. Resano and F.  
Vanhaecke, *J. Anal. At. Spectrom.*, 2013,  
**28**, 33–39.
- 40 D. P. Bishop, D. Clases, F. Fryer, E.  
Williams, S. Wilkins, D. J. Hare, N. Cole, U.  
Karst and P. A. Doble, *J. Anal. At.*  
*Spectrom.*, 2016, **31**, 197–202.
- 41 S. Kulaksiz and M. Bau, *Earth Planet. Sci.*  
*Lett.*, 2013, **362**, 43–50.
- 42 K. L. Linge and K. E. Jarvis, *Geostand.*  
*Geoanalytical Res.*, 2009, **33**, 445–467.
- 43 M. P. Elizalde-González, E. García-Díaz,  
M. González-Perea and J. Mattusch,  
*Environ. Sci. Pollut. Res.*, 2017, **24**, 8164–  
8175.